Journal of Harbin Engineering University
ISSN: 1006-7043

Vol 45 No. 7
July 2024

Investigation of Thermoacoustic Refrigeration System for Three Different Stack Geometry with Helium Gas.

Kamlesh S Shelke[1], Dr. Uday S Wankhede[2]
[1]Research Scholar, Government College of Engineering, Chandrapur,
Gondwana University, Gadchiroli, Maharashtra, India
[2]Associate Professor, Government College of Engineering, Nagpur,
Nagpur University, Nagpur, Maharashtra, India

Abstract: Numerous devices now in use could soon undergo a revolution because to recent advancements in the field of thermal acoustics. The thermo acoustic devices don't include any hazardous chemicals or environmentally hazardous materials which are feature of modern refrigeration systems. In this research work, an experimental investigations are conducted using polynamide nylon 6 material for stack and helium gas as working fluid. For making solid foundation of the research work the three different stack geometry are studied and the performance comparison done on the aspect of coefficient of performance (COP) and the temperature differential occurs on both ends of the stack. The expérimentation done with a range of optimum drive pressure of 6 to 10 bar and a constant frequency of 500Hz. The spiral, parallel plate and honeycomb geometry of the stack is used. The two parameter are analysed with the working frequency, operating pressure, and cooling load. The end results of this investigation suggest that the incorporation of helium gas and honeycomb stack in TARs can lead their performance, potentially opening up new avenues for applications in refrigeration and cooling technologies.

Keywords: Helium, honeycomb, parallel plate, polyamide nylon-6,spiral, thermo acoustic

Introduction

In conjunction with pressure variations, acoustic waves experience displacement and temperature oscillations. These oscillations generates a thermoacoustic effect, which enables the transfer of heat to or from the surface. A stack of parallel plates that are closely spaced is inserted into the thermo acoustic device to create a solid surface. Sound waves are generated when substantial temperature gradients are established throughout the stack, resulting in the generation of acoustic power and the formation of a thermoacoustic engine. Heat is generated when the gradient at a wall is negligible or nonexistent.

Modern life style now considers refrigerators to be essential. Modern refrigerators mostly employ the vapor compression refrigeration system, which is extremely effective but uses dangerous refrigerants hydro fluorocarbons (HFCs), which are depleting ozone substances and a major source of worry. Additionally, it has moving components that unquestionably shortens service life and lengthens maintenance. So, in this case, an attempt is made to replace the old refrigeration system and make it more environmentally friendly and provide effective refrigeration that would be both economical and maintenance-free while it's functioning at its best.

There is no need for environmentally risky refrigerants; only environmentally suited and safe inert gases are employed. The international ban on CFC (chlorofluorocarbon) use and the lack of confidence in CFC substitutes provide thermo acoustic devices a significant advantage over conventional freezers. The gases employed in these devices (such as air, helium, and xenon) have no greenhouse effect and are safe for the ozone layer. It is anticipated that rules on greenhouse gases would become stricter soon. Researchers had to come up with an alternative solution to this issue because of the restriction on the manufacture of CFCs and understanding of the harmful effects of CFCs on ozone depletion. Thermo acoustic refrigerator might be the best option in this situation to replace the traditional refrigeration systems. Additionally, the thermal acoustic cycle is well-suited to a proportional control model that is more efficient. The combination of all of these factors renders thermo acoustic refrigerators potentially alluring for widespread use.

Design methodology.

Basic of refrigeration:

The refrigerant is the operating fluid employed in refrigerators. The first and second laws of thermodynamics are the foundation of the refrigeration process and its operation. The vapour-compression cycle is the refrigeration cycle that is employed most frequently. In the vast majority of refrigeration units, including refrigerator heat pumps, air conditioners, and so forth, the fundamental operational cycle is the vapour compression cycle.

Acoustic Effect

Thermo acoustic wave oscillations include temperature oscillations, displacement oscillations, and pressure variations. Oscillations in a gas exhibiting the these three phenomena are expected to occur close to the solid surface to produce thermo acoustic effects. The interaction of these oscillations produces sound waves that are persistent in the presence of large temperature differences other than the surface of a solid. Acoustic theory pertains to the investigation of acoustic disturbances that propagate over extended distances. The expansion and compression of gas medium generate longitudinal acoustic vibrations. The direction of wave propagation is parallel to the particle movement in a longitudinal wave, suggesting that the particles oscillate back and forth around their respective equilibrium positions.

Parts Of Thermo Acuostic Refrigertaio System

1. STACK : The stack is the most critical element of thermoacoustic system, as it was location where phenomenon of thermoacoustic transpires. Consequently, the thermo acoustic device's efficacy is substantially influenced by the stack's characteristics. Material that is heaped should possess a high heating capacity and a lower thermal conductivity. In this design polynamide nylon 6 material is used for making parallel plate stack.
2. WORKING FLUID : The working fluid made major impact on the performance of the thermo acoustic refrigeration system. To obtain high efficiency and high power, high sound speed. high heat capacity ratio, mostly inert gases is used as working medium. When sound velocity increases in working fluid thermo acoustic power also increases, hence lighter gases which have high sound velocity can be used. The lighter gases like heliun, neon, argon can be used as working medium.
3. ACOUSTIC DRIVER: In this study the function generator of Aplab model no MSG1M is utilized to create the acoustic wave of different frequencies of range 0.1 Hz to 1 MHz, to drive the acoustic driver. To increase the power input of thermo acoustic refrigeration system, it is require to amplify the power input of acoustic driver and to do this an amplifier of Ahuja SSA 5000EM of maximum power 30 watts is utilized.
4. RESONATOR : It is a longer tube in which a stack of specified geometry and two heat exchangers are installed. It can be made of differnt material like glass, acrylic. The material of resonator should be such that it should withstand the high frequency.

Design Procedure

The thermo-acoustic refrigeration system, as determined by MEH Tijani [1], necessitates the determination of numerous parameters with predetermined values for specific purposes, including:

1. Average Pressure: Mechanical strength of the resonator is determined by average pressure. Leakages are mitigated by the elevated average pressure.
2. Frequency: The high frequency selected for prolongation of sound and for great efficiency of driver.
3. Cooling load: This is the refrigerating effect which may be obtained from the thermo acoustic refrigeration system.
4. Working gas: The working fluid should be such that the experimentation obtains high efficiency and high power, and high sound speed.
5. Stack material: It should possess a higher specific heating capacity and limited thermal conductivity. Hence considering the design aspect of above following parameters have fixed for designing:

1. Average pressure (p_m = 10 bar)
2. Frequency 500Hz (Optimized Value)
3. Cooling load
4. Working fluid (Helium gas)

5. Mean Temperature. ($T_m=27^0C$)

6. Stack material with high specific heat capacity and low thermal conductivity, so Polyamide Nylon 6 material is selected.

Nomenclature:

β	Thermal expansion coefficient	$[K^{-1}]$
γ	Ratio, isobaric to isochoric specific heats	
δ_k	thermal penetration depth of gas	[m]
δ_v	viscous penetration depth of gas	[m]
λ	Wave length	[m]
μ	dynamic viscosity	[Pa.s]
ν	kinematic viscosity	$[m^2/s]$
ρ_m	density	$[kg/m^3]$
ω	angular frequency	[rad/s]
C_p	specific heat capacity	[J/kg.K]
$2y_0$	stack plate spacing	[m]
x_s	position of the stack	[m]
$2l$	stack plate thickness	[m]
a	sound velocity of gas	[m/s]
f	frequency	[Hz]
T_h	Hot heat exchanger temperature	[K]
T_c	Cold heat exchanger temperature	[K]
T_m	Mean temperature	[K]
ΔT_m	Temperature gradient	
K_v	Wave number	
D	Drive ratio	
B	Blockage Ratio	
L	Resonator length	[m]
δ_{kn}	normalized thermal penetration depth of gas	
X_s	Stack center position	[m]
L_s	Length of stack	[m]
X_N	Normal Stack position	[m]
L_{SN}	Normal Stack length	[m]
σ	Prandtl Number	
Po	Dynamic Pressure amplitude	
Pm	Average Pressure	
Q_{cn}	Cooling power	[W]
W_n	Acoustic power	[W]

1. Stack Design

How much heat may diffuse through a gas layer in half a cycle of oscillations is called the thermal penetration depth. mThe viscous penetration depth δv is thickness of stratum at which the viscosity effect is most pronounced near the boundaries.

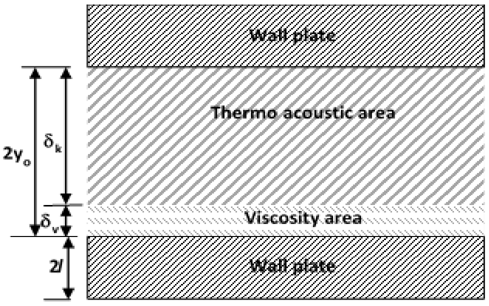

Figure.1 Illustration of the area δ_k and δ_v on the stack channel

$$\delta_k = \sqrt{\frac{2K}{\rho_m x C_p x \omega}}$$

$\delta_k = 0.336$ mm

$$\delta v = \sqrt{\frac{2\mu}{\rho_m x \omega}}$$

$\delta_v = 0.2788$ mm

2. Stack Spacing:

The distance between the frames or the air channel is denoted as (2yo).

$2y_o = 3 \times \delta_k$

$y_o = 0.504$ mm

3. Stack plate thickness:

It can be calculated as: $2l = 2yo\left(\frac{1}{B} - 1\right)$

The value of plate thickness will be **2mm**.

4. Stack Position:.

The stack position should be situated at a distance of λ/20 of the acoustic wavelength from the close end of the resonator in order to achieve the maximum cooling power.

$$x_s = \frac{\lambda}{20}$$

$x_s = 0.034$m

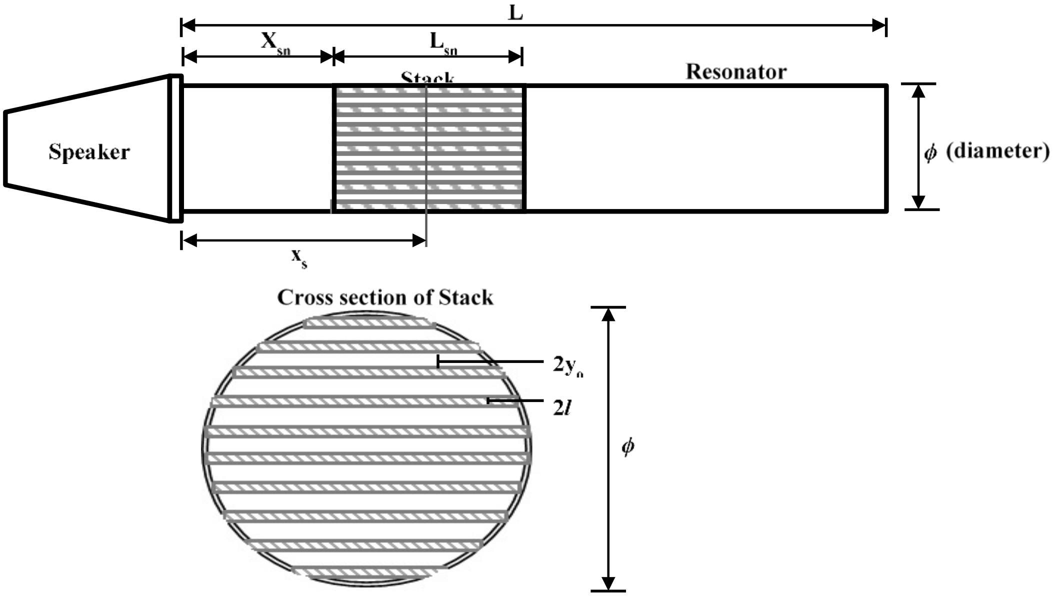

Figure.2. Illustration of various parameters and specification with geometry .

5. Resonator Length:

The minimal L resonator length for the closed tube side is typically λ / 4.

$$\lambda = \frac{a}{f} \qquad L = \frac{\lambda}{4}$$

λ = 0.68058m, L= 0.170145 m

6. Drive ratio:

Since the power density is directly related to average mean pressure and drive ratio, it is ideal to have high values for these parameters. So here it is considered as 3%.

$$D = \frac{P_0}{P_m}$$

D = 0.03

7. Blockage Ratio:

The presentation of the total area between the solid and gas areas will be elucidated by this parameter. It can also be termed as stack porosity. If this porosity increases then thermo acoustic area will decrease.

$$B = \frac{y_0}{y_0 + l}$$

It can be calculated as **B =0.834437**

8. Normalized thermal penetration depth: $\delta_{kn} = \frac{\delta_k}{y_0}$

δ_{kn} = 0.264344

9. Normal Stack Position: $X_N = K_v \times X_s$

X_N = 0.184003

10. Normal Stack length: $L_{SN} = K_v \times L_s$

L_{SN}= 0.276005

Experimental Set Up

Figure 3 Experimental Set Up of Thermo Acoustic Refrigeration System

Figure 4 Stack geometry spiral, parallel and honeycomb

Experimental Procedure

1. The experimental set up comprises of cold and hot heat exchangers, acoustic driver housing, stack, acoustic driver, a resonator occupied with operating fluid.
2. The acoustic driver creates pressure wave and its magnitude is measured by pressure transducer.
3. The charging pressure is measured with bourdon tube pressure gauge.
4. For measurement of temperature in hot and cold heat exchanger's thermocouples are employed.
5. After switching on the power supply, and set the desired frequency in signal generator its start functioning and generate standing acoustic wave with the help of acoustic driver.
6. Each side of the stack experiences a temperature differential, which is then recorded in the heat exchanger's cold and hot sides.

Result and Discussion

The thermo acoustic refrigeration system with three different stack and helium as a working fluid being studied under different working pressure at a difference viz. 6 bar, 7 bar, 8 bar, 9 bar, and 10 bar. Because after every 1 bar pressure it gives significant results and the time step for the performance were considered as a 5min. The effect of these conditions on the performance parameters hot and cold end temperature of stack of the system and the same with coefficient of performance is discussed here.

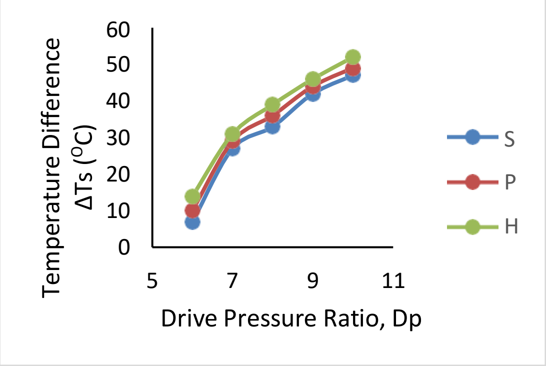

Figure 5 Effect of drive pressure ratio on temperature difference between two end of stack

The fig. 5 illustrates the effect of Drive Pressure (Dp) on the Temperature Difference (ΔTs) between the two ends of three stack configurations viz. Spiral (S), Parallel (P), and Honeycomb (H) using helium as the working fluid. As the Drive Pressure Ratio increases, the Temperature Difference (ΔTs) also increases for all configurations, indicating a greater thermal gradient is achieved at higher pressure ratios. By the time the Drive Pressure Ratio reaches 10 bar, the temperature difference for the Honeycomb stack is the highest at about 55°C, followed closely by the Parallel stack at around 50°C, and the Spiral stack at about 48°C. This demonstrates that while the Honeycomb stack consistently provides the highest thermal gradient, the differences between the configurations become less pronounced at higher pressure ratios.

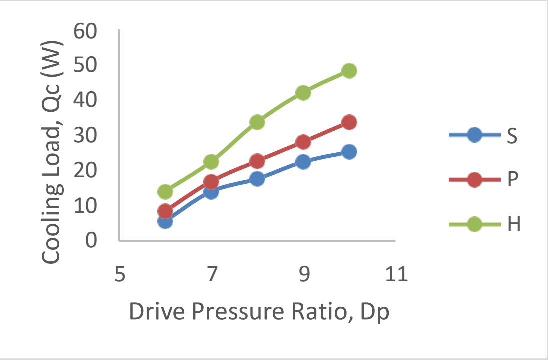

Figure 6 The impact of the drive pressure ratio on the cooling load

The fig. 6 shows the impact of the drive pressure ratio on the cooling load, between drive pressure ratios of 8 and 10 bar, the Cooling Load continues to increase for all configurations. By a Drive Pressure Ratio of 10 bar, the Honeycomb stack achieves the highest cooling load, reaching approximately 50 W. The Parallel stack follows with about 35 W, and the Spiral stack achieves around 30 W.

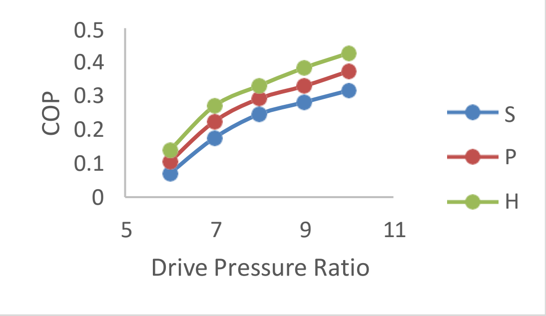

Figure 7 Effect of drive pressure ratio on coefficient of performance

The fig.7 illustrates the experimental investigations that, among all the stack configurations, the Honeycomb (H) stack consistently demonstrates the highest COP, starting at around 0.16 at a Drive Pressure Ratio of 5 and rising to approximately 0.42 at a ratio of 10. The Parallel (P) stack shows intermediate performance, beginning at about 0.11 and increasing to around 0.33 over the same range. The Spiral (S) stack exhibits the lowest COP, starting at roughly 0.08 and reaching approximately 0.26 at the highest Drive Pressure Ratio.

Conclusions

1. When the charging pressure is low, the working fluid displacement is low, which results in a lower heat transfer rate.
2. When the charging pressure is high, the working fluid displacement is also high, which results in an enhanced heat transfer rate.
3. The occurrence of lowest temperature is different for at different charging pressure.
4. The maximum lowest temperature occurs at highest charging pressure.
5. The maximum COP occurs at highest charging pressure.
6. Thus for obtaining the optimal value of COP in any stack geometry the charging pressure should be high (i.e. around 10 bar) and the operating frequency must be high (i.e. around 500 Hz).
7. This analysis highlights the efficiency of working fluid Helium and various stack geometries, indicating that for maximum COP with Honeycomb stack geometry is optimal.

References

[1] M. E. H. Tijani, J. C. H. Zeegers, and A. De Waele, “The optimal stack spacing for thermoacoustic refrigeration,” *J. Acoust. Soc. Am.*, vol. 112, no. 1, pp. 128–133, 2002.

[2] S. L. Garrett, J. A. Adeff, and T. J. Hofier, “Thermoacoustic refrigerator for space applications,” in *Journal of Thermophysics and Heat Transfer*, Oct. 1993, vol. 7, no. 4, pp. 595–599. doi: 10.2514/3.466.

[3] N. A. Zolpakar, N. Mohd-Ghazali, and M. H. El-Fawal, “Performance analysis of the standing wave thermoacoustic refrigerator: A review,” *Renew. Sustain. energy Rev.*, vol. 54, pp. 626–634, 2016.

[4] F. Zink, J. S. Vipperman, and L. A. Schaefer, “Environmental motivation to switch to thermoacoustic refrigeration,” *Appl. Therm. Eng.*, vol. 30, no. 2–3, pp. 119–126, 2010.

[5] I. A. Ramadan, H. Bailliet, G. Poignand, and D. Gardner, “Design, manufacturing and testing of a compact thermoacoustic refrigerator,” *Appl. Therm. Eng.*, vol. 189, p. 116705, 2021.

[6] M. A. Alamir, “An artificial neural network model for predicting the performance of thermoacoustic refrigerators,” *Int. J. Heat Mass Transf.*, vol. 164, p. 120551, 2021.

[7] T. Jin, R. Yang, Y. Wang, Y. Feng, and K. Tang, “Acoustic field characteristics and performance analysis of a looped travelling-wave thermoacoustic refrigerator,” *Energy Convers. Manag.*, vol. 123, pp. 243–251, 2016.

[8] A. C. Alcock, L. K. Tartibu, and T. C. Jen, “Experimental investigation of an adjustable thermoacoustically-driven thermoacoustic refrigerator,” *Int. J. Refrig.*, vol. 94, pp. 71–86, 2018.

[9] J. Chi, J. Xu, L. Zhang, Z. Wu, J. Hu, and E. Luo, “Study of a gas-liquid-coupled heat-driven room-temperature thermoacoustic refrigerator with different working gases,” *Energy Convers. Manag.*, vol. 246, p. 114657, 2021.

[10] L. K. Tartibu, “Developing more efficient travelling-wave thermo-acoustic refrigerators: A review,” *Sustain. Energy Technol. Assessments*, vol. 31, pp. 102–114, 2019.

[11] B. G. Prashantha, G. Narasimham, S. Seetharamu, and K. Manjunatha, “Effect of gas blockage on the theoretical performance of thermoacoustic refrigerators,” *Int. J. Air-Conditioning Refrig.*, vol. 29, no. 03, p. 2150026, 2021.

[12] I. Setiawan, M. Nohtomi, and M. Katsuta, “Critical temperature differences of a standing wave thermoacoustic prime mover with various helium-based binary mixture working gases,” in *Journal of Physics:*

Conference Series, 2015, vol. 622, no. 1, p. 12010.

[13] N. V Shivakumara and A. Bheemsha, “Performance Analysis of Thermoacoustic Refrigerator of 10 W Cooling Power made up of Poly-Vinyl-Chloride for Different Parallel Plate Stacks by using Helium as a Working Fluid,” *J. Therm. Sci.*, vol. 30, pp. 2037–2055, 2021.

[14] A. Krstic *et al.*, “Designing and manufacturing a thermoacoustic refrigerator,” *JUEPPEQ J. Undergrad. Eng. Phys. Phys. Exp. Queen’s*, vol. 1, pp. 1–17, 2020.

[15] N. A. Zolpakar, N. Mohd-Ghazali, and R. Ahmad, “Single-objective optimization of a thermoacoustic refrigerator,” in *Applied Mechanics and Materials*, 2016, vol. 819, pp. 88–93.

[16] N. Rott, “Thermoacoustics,” in *Advances in Applied Mechanics*, vol. 20, C.-S. B. T.-A. in A. M. Yih, Ed. Elsevier, 1980, pp. 135–175. doi: 10.1016/S0065-2156(08)70233-3.

[17] M. E. Poese and S. L. Garrett, “Performance measurements on a thermoacoustic refrigerator driven at high amplitudes,” *J. Acoust. Soc. Am.*, vol. 107, no. 5, pp. 2480–2486, May 2000, doi: 10.1121/1.428635.

[18] J. R. Belcher, W. V. Slaton, R. Raspet, H. E. Bass, and J. Lightfoot, “Working gases in thermoacoustic engines,” *J. Acoust. Soc. Am.*, vol. 105, no. 5, pp. 2677–2684, May 1999, doi: 10.1121/1.426884.

[19] M. Wetzel and C. Herman, “Design optimization of thermoacoustic refrigerators,” *Int. J. Refrig.*, vol. 20, no. 1, pp. 3–21, Jan. 1997, doi: 10.1016/S0140-7007(96)00064-3.

[20] T. Gajbhiye, S. Shelare, and K. Aglawe, “Current and Future Challenges of Nanomaterials in Solar Energy Desalination Systems in Last Decade,” *Transdiscipl. J. Eng. Sci.*, vol. 13, pp. 187–201, Dec. 2022, doi: 10.22545/2022/00217.

[21] H. Bailliet, P. Lotton, M. Bruneau, V. Gusev, J.-C. Valiere, and B. Gazengel, “Acoustic power flow measurement in a thermoacoustic resonator by means of laser Doppler anemometry (LDA) and microphonic measurement,” *Appl. Acoust.*, vol. 60, pp. 1–11, Jan. 2000.

[22] M. E. . Tijani, J. C. . Zeegers, and A. T. A. . de Waele, “Design of thermoacoustic refrigerators,” *Cryogenics (Guildf).*, vol. 42, no. 1, pp. 49–57, Jan. 2002, doi: 10.1016/S0011-2275(01)00179-5.

[23] K. Tang, G. B. Chen, T. Jin, R. Bao, B. Kong, and L. M. Qiu, “Influence of resonance tube length on performance of thermoacoustically driven pulse tube refrigerator,” *Cryogenics (Guildf).*, vol. 45, no. 3, pp. 185–191, Mar. 2005, doi: 10.1016/j.cryogenics.2004.10.002.

[24] Q. Tu, V. Gusev, M. Bruneau, C. Zhang, L. Zhao, and F. Guo, “Experimental and theoretical investigation on frequency characteristic of loudspeaker-driven thermoacoustic refrigerator,” *Cryogenics (Guildf).*, vol. 45, no. 12, pp. 739–746, 2005, doi: https://doi.org/10.1016/j.cryogenics.2005.09.004.

[25] Y. A. Abakr, M. Al-Atabi, and C. Baiman, “The influence of wave patterns and frequency on thermo-acoustic cooling effect,” *J. Eng. Sci. Technol.*, vol. 6, no. 3, pp. 394–398, 2011.

[26] C. Herman and Z. Travnicek, “Cool sound: the future of refrigeration? Thermodynamic and heat transfer issues in thermoacoustic refrigeration,” *Heat Mass Transf.*, vol. 42, no. 6, pp. 492–500, Apr. 2006, doi: 10.1007/s00231-005-0046-x.

[27] M. E. H. Tijani, J. C. H. Zeegers, and A. T. A. . de Waele, “Construction and performance of a thermoacoustic refrigerator,” *Cryogenics (Guildf).*, vol. 42, no. 1, pp. 59–66, 2002, doi: https://doi.org/10.1016/S0011-2275(01)00180-1.

[28] B. Ramesh Nayak, G. Pundarika, and B. Arya, “Influence of stack geometry on the performance of thermoacoustic refrigerator,” *Sādhanā*, vol. 42, no. 2, pp. 223–230, 2017, doi: 10.1007/s12046-016-0585-5.

[29] B. G. Prashantha, M. S. G. Gowda, S. Seetharamu, and G. S. V. L. Narasimham, “Design Analysis of Thermoacoustic Refrigerator Using Air and Helium as Working Substances,” *Int. J. Therm. Environ. Eng.*, vol.

13, no. 2, pp. 113–120, 2017, doi: 10.5383/ijtee.13.02.006.

[30] K. Ghorbanian and M. Karimi, "Design and optimization of a heat driven thermoacoustic refrigerator," *Appl. Therm. Eng.*, vol. 62, pp. 653–661, Jan. 2014, doi: 10.1016/j.applthermaleng.2013.09.058.

[31] B. G. Prashantha, G. S. V. L. Narasimham, S. Seetharamu, and V. B. Hemadri, "Theoretical evaluation of stack-based thermoacoustic refrigerators," *Int. J. Air-Conditioning Refrig.*, vol. 30, no. 1, p. 8, 2022, doi: 10.1007/s44189-022-00008-2.

[32] B. Arya, B. Ramesh Nayak, and N. V Shivakumara, "Effect of Dynamic Pressure on the Performance of Thermoacoustic Refrigerator with Aluminium (Al) Resonator," *IOP Conf. Ser. Mater. Sci. Eng.*, vol. 346, no. 1, p. 12034, 2018, doi: 10.1088/1757-899X/346/1/012034.